MATERIAL POINT METHOD FOR RUN-OUT ANALYSIS OF EARTHQUAKE-INDUCED LONG-TRAVELING SOIL FLOWS

Muneyoshi NUMADA[1], Kazuo KONAGAI [2], Hironori ITO[3] and Jörgen JOHANSSON[4]

[1] PhD Candidate, Institute of Industrial Science, University of Tokyo
Tokyo 153-8505, Japan, numada@iis.u-tokyo.ac.jp
[2] Professor, Institute of Industrial Science, University of Tokyo
Tokyo 153-8505, Japan, konagai@iis.u-tokyo.ac.jp
[3] Ms. Candidate, Institute of Industrial Science, University of Tokyo
Tokyo 153-8505, Japan, itouhrnr@iis.u-tokyo.ac.jp
[4] PhD Candidate, Research Associate, Institute of Industrial Science, University of Tokyo
Tokyo 153-8505, Japan, jorgen@iis.u-tokyo.ac.jp

Landslides can range in size from small movements of loose debris to massive collapses of entire summits. For short to medium-length slopes, some measures will be effective for assessing and mitigating landslide hazards. Extremely large slope failures, however, are very difficult to mitigate, and the importance of run-out analysis emerges. Lagrangian Particle Finite Difference Method (LPFDM) is extended to handle rapid and long-traveling flows of soil. LPFDM describes a soil mass as a cluster of Lagrangian material points that carry all necessary information of the material and move freely across a Eulerian grid where the equations of motion are solved.

Key words: *Large deformations of soils, Lagrangian particle, Eulerian grid*

1. INTRODUCTION

Landslides can range in size from small movements of loose debris to massive collapses of entire summits. For short to medium-length slopes, installing preventive drainage works, anchoring and/or reinforcing slopes will be effective for assessing and mitigating landslide hazards. Extremely large slope failures, however, are very difficult to mitigate, and thus the importance of run-out analysis emerges. Many landslides with limited internal deformation will move as coherent masses on thin mobile basal layers. Others, however, will become flow-like in character after running some long distances, though exhibiting some solid features at their early stages of failure.

For studying large deformations of soils, numerical methods such as FEM or FDM have been widely used. For example, the finite difference based FLAC (Fast Lagrangian Analysis of Continua)[1)] calculates large strains by using low-order strain elements. However, when dealing with large strains, highly distorted elements often account for inaccurate results.

In the field of computational fluid dynamics, where history-dependent materials are less common, purely Eulerian methods are often used. Sulsky et al.[2)] extended it further to solid mechanics. Their method evolved from a particle-in-cell (PIC) method is referred to as the Lagrangian Particle Method (LPM) or the Material Point Method (MPM). The MPM is categorized as one of the mesh-less methods formulated in an arbitrary Lagrangian-Eulerian description of motion. In MPM, a body to be analyzed is described as a cluster of material points. The material points, which carry all Lagrangian parameters, can move freely across cell boundaries of a stationary Eulerian mesh. This mesh, called a computational mesh, should cover the virtual position of the analyzed body. The computational mesh can remain constant for the entire computation, thus the main disadvantage of the conventional finite element method related to the problem of mesh distortions is eliminated.

Konagai and Johansson[3] developed two dimensional LPFDM (Lagrangian Particle Finite Difference Method) based on the LPM scheme of calculation. The method was intended to be a projection of FLAC formulations on the LPM scheme so that the present method allows for extremely large deformations of soils retaining the merits of FLAC. The method is further extended herein to model a rapid and long-traveling soil flow keeping its planar geometry.

2. MODELING OF LANDSLIDE MASS

Though the use of a three-dimensional model is a straightforward approach to the problem, the landslide mass flowing thin over a stiff base slope is modeled as a two-dimensional soil mat. The landslide mass is represented by a planner assemblage of soil columns (Material Points) contacting each other, free to deform and retaining fixed volumes in their descent down a curving path (**Figure 1**).

A cluster of material points representing the landslide mass slide on a thin mobile basal layer ($\xi-\psi$ plane in **Figure 1**). Cells of a computational Eulerian mesh on the $\xi-\psi$ plane are arranged in such a way that their projections on a horizontal *x*-*y* plane are a regular square mesh with sides parallel to *x* and *y* axes of the Cartesian coordinate system. Though the real slope is not a perfect plane, each cell is assumed to be small enough for the cell and its neighboring cells to be arranged in one plane. The cells on the $\xi-\psi$ plane are thus parallelograms. The orientation of the $\xi-\psi$ plane is described by ξ and ψ axes; the ξ axis is a horizontal line produced by the intersection of the $\xi-\psi$ plane and a horizontal plane, while the ψ axis describes the slope of the $\xi-\psi$ plane. LPFDM formulation on the $\xi-\psi$ plane is available in the reference (Konagai et al., 2002).

A soil column (material point) is assumed to experience the same strains in the $\xi-\psi$ plane over its entire height (z: 0-*h*). Excluding its weight, the stress components for the soil column, $\sigma_{xx,0}$, $\sigma_{yy,0}$ and $\tau_{xy,0}$ are kept unchanged over its height. However with the presence of its weight, realized stress components are described as:

$$\sigma_{xx}=\sigma_{xx,0}+K_0\gamma z,\quad \sigma_{yy}=\sigma_{yy,0}+K_0\gamma z \qquad \tau_{xy}=\tau_{xx,0}\quad \sigma_{zz}=\gamma z \qquad \text{(1a)-(1d)}$$

with

$$K_0=\frac{\nu}{1-\nu} \qquad \text{(1e)}$$

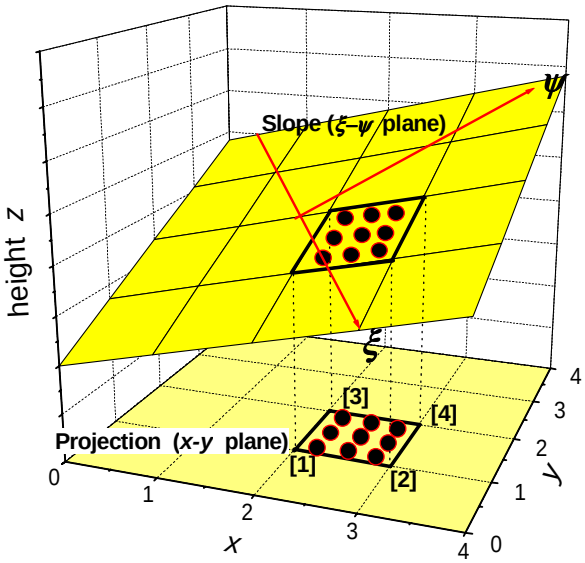

Figure 1. Material points showing landslide mass

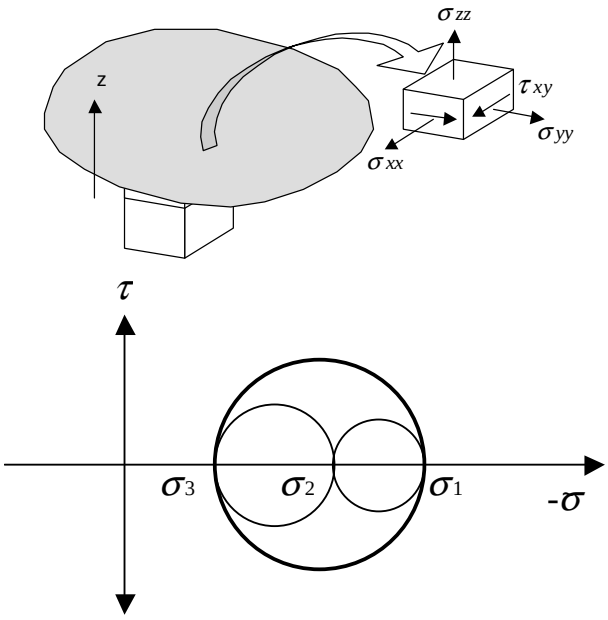

Figure 2. Soil column (above) following Mohr-Coulomb's criterion (below)

The above components are averaged over the column's height.

$$\tilde{\sigma}_{xx}=\frac{1}{h}\int_0^h\sigma_{xx}dz=\sigma_{xx,0}+\frac{1}{2}K_0\gamma h$$

$$\tilde{\sigma}_{yy}=\frac{1}{h}\int_0^h\sigma_{yy}dz=\sigma_{yy,0}+\frac{1}{2}K_0\gamma h \qquad \text{(2a)-(2d)}$$

$$\tilde{\tau}_{xy}=\tau_{xx,0}$$

$$\tilde{\sigma}_{zz}=\frac{1}{h}\int_0^h\sigma_{zz}dz=\frac{1}{2}\gamma h$$

Essentially, Mohr/Coulomb criterion should be used for a particular soil element that experiences homogeneous stresses over its entire size. For the averaged stress components, however, Mohr/Coulomb criterion is tentatively used herein for describing elasto-plastic features of the "material point". To draw a Mohr circle for the material point, the maximum and minimum principal stresses must be chosen among three principal stresses including $\tilde{\sigma}_{zz}$. For this, two principal stresses $\tilde{\sigma}_a$ and $\tilde{\sigma}_b$ in the *x*-*y* plane are first to be obtained. It is noted that differing from the geotechnical engineering customary to describe compressive stresses as positive, tensile stresses are expressed to be positive in LPFDM.

$$\tilde{\sigma}_a = \left(\frac{\tilde{\sigma}_{xx} + \tilde{\sigma}_{yy}}{2} + \sqrt{\left(\frac{\tilde{\sigma}_{xx} - \tilde{\sigma}_{yy}}{2} \right)^2 + \tilde{\tau}_{xy}^{\,2}} \right)$$
$$= \left(\frac{\sigma_{xx,0} + \sigma_{yy,0}}{2} + \sqrt{\left(\frac{\sigma_{xx,0} - \sigma_{yy,0}}{2} \right)^2 + \tau_{xy,0}^{\,2}} \right) + \frac{1}{2}\gamma h \qquad (3a)$$

$$\tilde{\sigma}_b = \left(\frac{\sigma_{xx,0} + \sigma_{yy,0}}{2} - \sqrt{\left(\frac{\sigma_{xx,0} - \sigma_{yy,0}}{2} \right)^2 + \tau_{xy,0}^{\,2}} \right) + \frac{1}{2}\gamma h \qquad (3b)$$

Among the three principal stresses, the maximum, intermediate and minimum principal stresses are determined as:

$$\sigma_1 = \max(-\tilde{\sigma}_a, \; -\tilde{\sigma}_b, \; -\tilde{\sigma}_{zz}) \qquad (4a)$$
$$\sigma_2 = \text{intermediate}(-\tilde{\sigma}_a, \; -\tilde{\sigma}_b, \; -\tilde{\sigma}_{zz}) \qquad (4b)$$
$$\sigma_3 = \min(-\tilde{\sigma}_a, \; -\tilde{\sigma}_b, \; -\tilde{\sigma}_{zz}) \qquad (4c)$$

Once the Mohr circle intersects the failure envelope, stresses are "reduced" in such a way that the reduced stress make up a slightly reduced Mohr circle that touches the envelope.

3. NUMERICAL EXAMPLES

Both the internal friction angles and the cohesions for Lagrangian points were modified to fluctuate randomly around their mean values so that the deviations eventually exhibit the Gaussian distributions. This manupulation is based on the idea that a material exhibiting a complicated hysterisis is comprised of a number of elements exhibiting simple and ideal features. Parameters (mean values) for the material used in the following example are listed in **Table 1**. Standard deviations of the fluctuated parameters were set at 33% of their mean values.

Table 1. Lagrangian parameters

Young's modulus:	5×10^7 N/m^2
Poisson's ratio:	0.30
Density:	1700 kg/m^3
Internal friction angle:	0.5 rad
Cohesion:	9800 N/m^2
Strength reduction:	Both cohesion and Internal friction angle are reduced by 50%
Initial friction angle on the slip surface	0.5 rad
u_{ref} in Equation (9)	0.1 m
α for local non-viscous damping	0.8
L: Cell size on x-y plane	1m

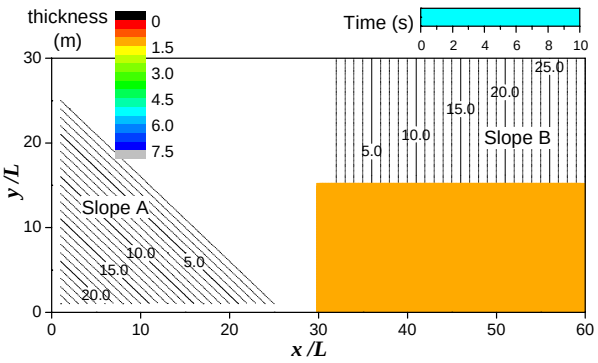

(**a**) t = 0 s

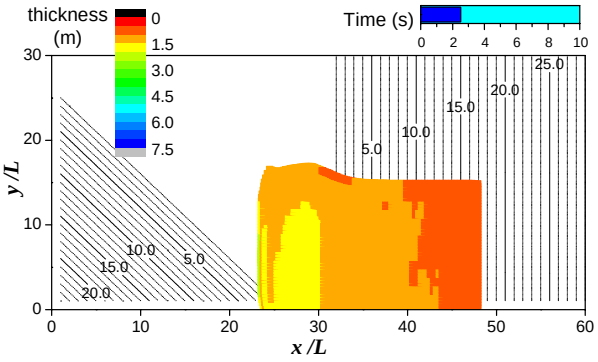

(**b**) t = 2.5 s

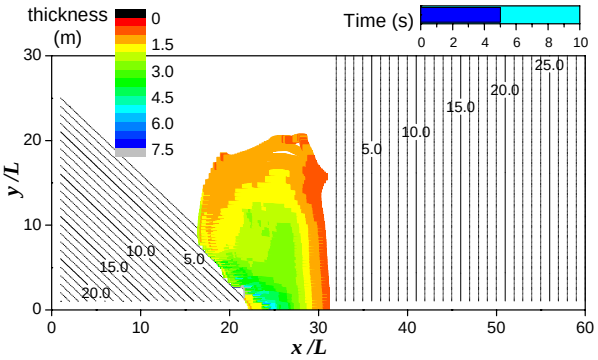

(**c**) t = 5.0 s

Figure 3. Long-traveling soil flow
(**Click here** for a 432kB GIF animation)

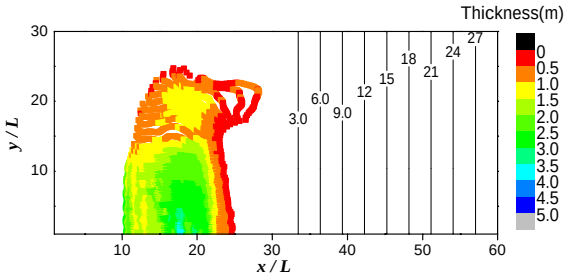

(**a**) Thickness changes of the soil mass

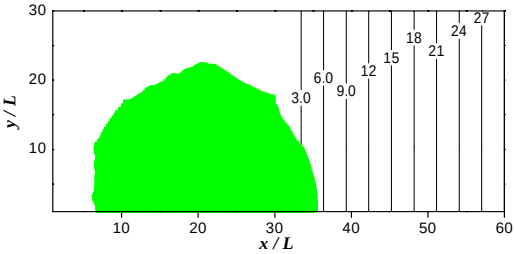

(**b**) Thickness constant of the soil mass

Figure 4. Comparison of travel distance

The slope discussed herein is described as a combination of different planes intersecting with each other. The uppermost surfaces of these planes define the slope configuration. **Figures 3a-3c** show the plan of the slope. Contour lines in this figure show that there are two slopes **A** and **B** making up the configuration. Diagonal contour lines on the left show that Slope **A** goes diagonally down to the right, while contour lines to the right describe that Slope **B** dips 45 degrees leftward. Lagrangian points are initially arranged in square on Slope **B**. The gravitational acceleration was then given at once to the soil mass, and the mass started sliding the slope under its own weight (**Figures 3a-3d**). The head of the landslide mass slows down to block the motion of its tail when it reaches the flat land causing the soil at the toe of **Slope B** to be pushed up by the tail. With no lateral confinement on its edge, the soil mass spreads wide as it surged across the horizontal plane, and after hitting Slope **A**, the direction of the mass flow turned avoiding Slope **A**.

Figure 4 compares travel distances for two landslides with the same constitutive properties moving to the left and down along a 45 degrees slope. The thickness of soil mass in **Figure 5b** is assumed to remain constant due to a strong restraint from plant roots, whereas the soil mass in **Figure 4a** is the same as that examined in **Figure 3**, and changes its thickness freely.

The analysis shows that travel distance of the soil mass in **Figure 4b** is longer than the mass in **Figure 4a**. Difference in energy loss accounts for the difference of travel distances. The thickness change of the soil mass in **Figure 4a** reduced the kinetic energy.

4. SUMMARY AND DISCUSSIONS

The previous example provided a perspective on the capability of the present method for describing long-traveling soil flows. The landslide mass is represented by a planner assemblage of soil columns (Material Points) contacting each other, free to deform and retaining fixed volumes in their descent down a curving path.

The method however leaves much to improve by comparing these numerical simulations with real examples. Because all Lagrangian parameters for the entire landslide mass are hardly obtained. For example, it is quite often that plants growing on a landslide mass shoot their roots all through the soil mass in such a way that the overall characteristics of the soil mass is largely different from those obtained through conventional soil tests. One possible way will be to consider a real landslide as a huge “simple shear test”. In the “real-size” simple shear test, the distal end and surface configuration of the landslide mass can be clearly measured. If the landslide mass exhibits some liquefiable features, possible peak velocity of the landslide mass will be estimated from mud spatters remaining on walls, tree trunks etc. assuming that they follow forms of parabola

Differing from a conventional 2D model for run-out analysis, the model proposed herein allows the effect of energy consumption within the deformed landslide mass to be reflected on the numerical evaluation of travel distances(**Figure 4**). Once a good agreement with a real travel distance is obtained in a landslide-prone area through a parametric study, it is expected the result will provide necessary pieces of information for the landslide risk assessment in this area. An extension of this study will be addressed in future publications.

REFERENCES

1) Cundall, P.A. and Board, M.: A microcomputer program for modeling large-strain plasticity problems, *Numerical Methods in Geotechnics (Proc., 6th Int. Conf., Innsbruck, Austria, April 1988*), pp. 2101-2108. 1988.

2) Sulsky, D., Z., Chen, and H. L., Schreyer: A particle method for history dependent materials, *Comput. Methods Appl. Mech. Engrg*., **118**, 179-196, 1994.

3) Konagai, K. and J., Johansson: Two Dimensional Lagrangian Particle Finite Difference Method for Modeling Large Soil Deformations, *Structural Eng./ Earthquake Eng.* **18(2)**, 91s-95s, 2001.

(Received Oct 10, 2003)